

Extreme Confinement of Xenon by Cryptophane-111 in the Solid State**

Akil I. Joseph, Saul H. Lapidus, Christopher M. Kane, and K. Travis Holman*

Abstract: Solids that sorb, capture and/or store the heavier noble gases are of interest because of their potential for transformative rare gas separation/production, storage, or recovery technologies. Herein, we report the isolation, crystal structures, and thermal stabilities of a series of xenon and krypton clathrates of (\pm)-cryptophane-111 (**111**). One trigonal crystal form, $\text{Xe@111}\cdot\text{y}(\text{solvent})$, is exceptionally stable, retaining xenon at temperatures of up to about 300°C. The high kinetic stability is attributable not only to the high xenon affinity and cage-like nature of the host, but also to the crystal packing of the clathrate, wherein each window of the molecular container is blocked by the bridges of adjacent containers, effectively imprisoning the noble gas in the solid state. The results highlight the potential of discrete molecule materials exhibiting intrinsic microcavities or zero-dimensional pores.

The development of molecule-derived porous materials for the selective inclusion of the heavier noble gases is a growing area of research driven by the potential for transformative rare gas production or separation,^[1–4] probe,^[5] sensing^[6,7] recovery,^[8] and/or storage technologies. Xenon, in particular, is an expensive gas owing to its broad utility (such as in lighting, lasers, spacecraft propulsion, silicon etching (as XeF_2), anaesthesia, and NMR probes) and its low concentration in the atmosphere (87 ppb), requiring production by energy-intensive cryogenic distillation of large volumes of air. The cryogenic separation of Xe/Kr mixtures in rare gas production streams remains a critical stage of the production process that could perhaps be improved by sorption-based separation technologies. Moreover, mixtures of Xe/Kr (long-lived ^{85}Kr : $t_{1/2} = 10.8$ year, and short lived Xe isotopes) are also encountered in nuclear fuel reprocessing, and it has been proposed that the xenon recovered from spent nuclear fuel

could constitute a commercial source of the gas.^[1–4] Relatedly, there are as of yet no generally accepted waste forms for storage of ^{85}Kr , though sequestration in a stable solid form would be advantageous, as highlighted by recent efforts focusing on capture of gaseous iodine.^[9] Finally, the recovery of xenon from waste air streams is a recently commercialized swing sorption technology (Xecover) that may benefit from improved sorbents.^[8]

Concurrent with materials research aimed at rare gas inclusion are efforts toward optimizing xenon complexation in solution. Molecules that bind xenon hold promise for as-low-as picomolar detection limit hyperpolarized (HP) ^{129}Xe NMR based sensing technologies.^[6] To this end, the cryptophane-*nmm* family of molecular containers (Figure 1)

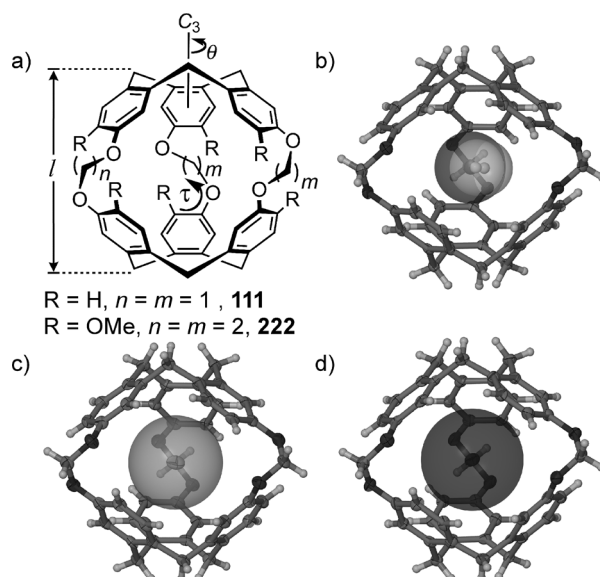


Figure 1. a) Cryptophanes **111** and **222**. b–d) Ellipsoid plots of the $\text{H}_2\text{O@111}$, Kr@111 , and Xe@111 complexes, respectively, from single-crystal structures of the triclinic clathrates $x(\text{guest})@111\cdot 1.5\text{DCE}$ ($x(\text{guest}) = \text{Xe}, 0.80\text{ Kr}, 0.50\text{ H}_2\text{O}$).^[27]

are the most actively studied hosts, owing to their unprecedented xenon affinities.^[10–15] Pioneered by Collet and co-workers, cryptophanes are cage-like molecules comprised of two cyclotribenzylene cups that are connected so as to enforce lipophilic cavities of tunable volumes.^[10] The (\pm)-cryptophane-222 (**222**) core structure has served as the platform for most cryptophane derivatives employed to date in sensing applications, with certain derivatives exhibiting room temperature xenon binding constants (K_a) approaching 10^5 in aqueous solutions.^[10–12] The smaller (\pm)-cryptophane-111

[*] A. I. Joseph, C. M. Kane, Prof. K. T. Holman
Department of Chemistry, Georgetown University
Washington, DC 20057 (USA)
E-mail: kth7@georgetown.edu

Dr. S. H. Lapidus
X-Ray Science Division, Argonne National Laboratory
9700 S Cass Ave, Lemont, IL 60439 (USA)

[**] This work was supported by the U.S. National Science Foundation (NSF; DMR-1106266, CHE-1337975). C.M.K. acknowledges the IMI Program of the NSF under DMR 0843934, and we thank Leonard Barbour for hosting C.M.K. at the University of Stellenbosch. Use of the National Synchrotron Light Source, Brookhaven National Laboratory, was supported by the U.S. Department of Energy, Office of Science, Office of Basic Energy Sciences, under DE-AC02-98CH10886.

Supporting information for this article is available on the WWW under <http://dx.doi.org/10.1002/anie.201409415>.

(**111**), however, exhibits a higher xenon affinity.^[13] The room temperature xenon binding constant of **111** in non-competitive (CDCl₃)₂ ($K_a \approx 10^4 \text{ L mol}^{-1}$) is over twice that of **222** ($K_a \approx 3000 \text{ L mol}^{-1}$).^[11] Derivatives of **111** for possible sensing applications are forthcoming,^[14,15] the first reported water-soluble derivative of **111** binds xenon with $K_a = 2.9(2) \times 10^4 \text{ L mol}^{-1}$ (298 K) in D₂O, as established by ¹²⁹Xe NMR spectroscopy.^[14]

Surprisingly, despite the high gas affinity of cryptophane hosts, and a figurative call-to-arms for the study of intrinsically porous cage-like molecular materials,^[16] the materials properties of empty cryptophanes or gas-filled cryptophane clathrates have not been much studied,^[17] particularly in the context of their potential for rare gas sorption/desorption or storage. Dmochowski and co-workers reported the crystal structures of members of the Xe@**222** family of complexes,^[12a] but no gas clathrates of **111** have yet been reported. A handful of other organic molecule complexes/clathrates of xenon (and a few of krypton) have been structurally characterized.^[1,2,18] We describe herein the isolation, crystal structures, and thermal stabilities of a series of racemic (\pm)-cryptophane-**111** (**111**) clathrates of xenon and krypton, one of which retains its xenon to temperatures of about 400 °C above the boiling point of the gas (−108 °C). The extreme, seemingly unprecedented, kinetic stability of the clathrate is attributable as much to the crystal packing as to the cage-like structure and xenon-complementarity of the host.

The only known crystal structures of **111** or its derivatives ($x\text{H}_2\text{O}@\mathbf{111} \cdot 2\text{CHCl}_3$ and its empty, metalated derivative $[(\eta^5\text{-C}_5\text{Me}_5\text{Ru})_6\mathbf{111}][\text{CF}_3\text{SO}_3]_6 \cdot x\text{NO}_2\text{Me}$) were reported by our group.^[14] The water complex and empty forms exhibit very different cryptophane conformations. In the empty, metalated form, the **111** core adopts a contracted conformation, characterized by a large twist of one orthocyclophane cup relative to the other ($\theta = 61(3)^\circ$), resulting in a short end-to-end length ($l = 7.4 \text{ \AA}$, defined by the methylene carbons of the cyclotribenzylenes), and a minimized cavity volume ($V_c = 32 \text{ \AA}^3$; Figure 1). In contrast, the partial water complex, $x\text{H}_2\text{O}@\mathbf{111} \cdot 2\text{CHCl}_3$, exhibits a less-twisted ($\theta = 18(1)^\circ$), fully expanded ($l \approx 8.4 \text{ \AA}$) conformation with a cavity measuring about 68 \AA^3 . Twisting of the **111** host is accomplished mainly by variations in the C_{Ar}–C_{Ar}–O–CH₂ dihedral angles (τ ; Figure 1), the closed form arising from an all antiperiplanar conformation ($\tau(\text{avg.}) = 177(2)^\circ$) and the open form arising from an all syn periplanar ($\tau(\text{avg.}) = 4(4)^\circ$) conformation. The OCH₂O methylenic carbons maintain planarity with the arene ring, optimizing conjugation with the oxygen non-bonded electrons. Notably, the expanded 68 \AA^3 cavity volume of $\text{H}_2\text{O}@\mathbf{111}$ compares favorably to that of Xe (42 \AA^3).

Crystals of $x\text{H}_2\text{O}@\mathbf{111} \cdot 2\text{CHCl}_3$ ^[14] were prepared by cooling a warm solution of **111** in CHCl₃. We now report that an isostructural xenon complex, $x\text{Xe}@\mathbf{111} \cdot 2\text{CHCl}_3$ ($0.5 < x < 1$), can similarly be obtained from xenon-treated CHCl₃ solutions. Single-crystal X-ray diffraction (SCXRD) revealed that the structure of $x\text{Xe}@\mathbf{111} \cdot 2\text{CHCl}_3$ ^[19] is indistinguishable from $x\text{H}_2\text{O}@\mathbf{111} \cdot 2\text{CHCl}_3$, except that xenon is found in place of encapsulated water. Unfortunately, poor crystal quality resulted in a poor structure refinement. Crystals of $x\text{Xe}@\mathbf{111} \cdot 2\text{CHCl}_3$ stored in CHCl₃ also seemed to convert

into a more stable phase. Difficulties in isolating and characterizing the above crystalline phases prompted us to explore alternative solvents and, ultimately, 1,2-dichloroethane (DCE) was chosen; **111** is more soluble in DCE and its higher boiling point allows for a greater differential solubility on heating/cooling.

Slow evaporation of a DCE solution of **111** yielded single crystals of a triclinic crystal form, $0.5\text{H}_2\text{O}@\mathbf{111} \cdot 1.5\text{DCE}$. SCXRD analysis at 100 K revealed that the **111** host exhibits near-*D*₃ symmetry and an open conformation nearly identical to that observed in $x\text{H}_2\text{O}@\mathbf{111} \cdot 2\text{CHCl}_3$, with $\tau(\text{avg.}) = 5(3)^\circ$, $\theta = 19(1)^\circ$, $l = 8.3 \text{ \AA}$ and $V_c = 69 \text{ \AA}^3$. Like $x\text{H}_2\text{O}@\mathbf{111} \cdot 2\text{CHCl}_3$, a single electron density peak in the cavity of the cryptophane was attributed to a partial occupancy water molecule. Apparently, in the absence of a more appropriate guest (DCE is too large for **111**),^[20] **111**, like **222**,^[11] scavenges water. Tandem thermogravimetric analysis mass spectrometry (TGA-MS, Figure 2a) of $0.5\text{H}_2\text{O}@\mathbf{111} \cdot 1.5\text{DCE}$ indicated loss of DCE (18.0%; $m/z = 63$ for vinyl chloride fragment) onsetting around 98 °C, followed by a nearly insignificant step at about 340 °C and sublimation/decomposition over 400 °C.

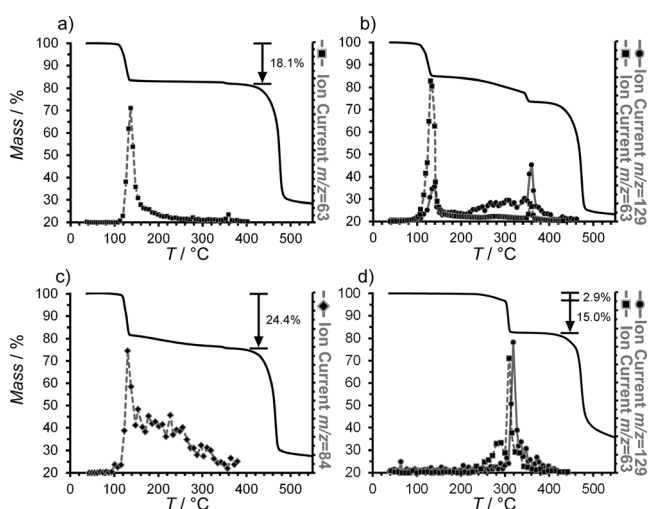


Figure 2. Tandem TGA-MS analysis of phase-pure crystal forms of **111**: a) triclinic $0.5\text{H}_2\text{O}@\mathbf{111} \cdot 1.5\text{DCE}$, b) isostructural $0.73\text{Xe}@\mathbf{111} \cdot 1.5\text{DCE}$, c) isostructural $0.80\text{Kr}@\mathbf{111} \cdot 1.5\text{DCE}$, and d) trigonal $\text{Xe}@\mathbf{111} \cdot 0.2\text{DCE}$. TGA curves are in black, whereas the curves with markers represent the MS ion current (arbitrary units) of guests (vinyl chloride, $m/z = 63$; xenon, $m/z = 129$; krypton $m/z = 84$).

Single crystals of a triclinic xenon-containing phase, $\text{Xe}@\mathbf{111} \cdot 1.5\text{DCE}$, were prepared by evaporation of a DCE solution of **111** within a closed vessel charged with xenon (Supporting Information, Figure S2). $\text{Xe}@\mathbf{111} \cdot 1.5\text{DCE}$ is structurally nearly identical to $0.5\text{H}_2\text{O}@\mathbf{111} \cdot 1.5\text{DCE}$, except that xenon is found in the **111** cavity instead of water (Supporting Information, Figure S13). The $\text{Xe}@\mathbf{111}$ complex (Figure 1d) exhibits an identical host conformation to the water complex, with $\tau(\text{avg.}) = 4(2)^\circ$, $l = 8.4 \text{ \AA}$, $\theta = 19(1)^\circ$, and $V_c = 70 \text{ \AA}^3$. The relative indifference in **111** conformations

between the Xe@**111** and H₂O@**111** complexes may be indicative of a steep barrier to conformational contraction of the host near the local energy minimum of the expanded conformation. The Xe atom is found perfectly centered in the **111** cavity and the 36 closest atoms to the xenon are the 36 arene carbon atoms of the host. Xe⋯C(arene) distances average 4.01(9) Å (3.86–4.20 Å), with the closest contacts being exactly at the sum of the van der Waals radii (3.86 Å) and the Xe⋯centroid(arene) distances measuring 3.77(3) Å. The Xe⋯centroid distances compare favorably to that of the Xe⋯C₆H₆ complex (3.77 Å) studied by microwave spectroscopy,^[21] suggesting nearly optimal Xe⋯arene interactions in Xe@**111**. In comparison, the known Xe@**222** complex (143 K) exhibits significantly longer Xe⋯C(arene) contacts, averaging 4.31(17) Å (4.03–4.77 Å), and Xe⋯centroid(arene) distances averaging 4.08(7) Å (Supporting Information, Tables S1,3, Figures S10,12). Perhaps counterintuitively, however, the Xe⋯H distances (important for xenon spin depolarization) involving the 36 protons of the Xe@**111** complex (4.35–6.19 Å) are greater than those involving the closest 36 protons of the Xe@**222** complex (3.65–5.76 Å), which is largely due to the conformation of the alkyldioxy linkers and the presence of methoxy groups in the latter (Supporting Information, Table S7,8). This contrasts with the somewhat longer T_1 relaxation time for xenon within **222** as compared to **111**.^[13]

The xenon exhibits a packing coefficient within the **111** cavity of $V_{\text{Xe}}/V_c \approx 0.62$, which is somewhat high for container complexes governed principally by dispersion interactions,^[22] and particularly for complexes of gases. The known Xe@**222** complex, on the other hand, exhibits a packing coefficient of $V_{\text{Xe}}/V_c = 42/89 \approx 0.47$, which is low for such complexes. Notably, the Xe@**111** complex appears to adopt nearly the most expanded achievable **111** conformation, yet the Xe⋯C contacts do not intrude on the van der Waals radii. This suggests the **111** cavity, in its most open conformation, is a near perfect fit for xenon. On the other hand, the Xe@**222** complex, with $V_c = 88 \text{ Å}^3$, adopts approximately the most contracted possible conformation of all known **222**-core complexes, wherein V_c varies widely from 84–119 Å³.^[12a,23] The data suggest that the **222** cavity is perhaps a bit large to optimize interactions with xenon.

The method of preparing crystals of Xe@**111**·1.5DCE concomitantly produced a fine powder of composition Xe@**111**· y DCE ($y \leq 1/2$); this material was later confirmed to be a trigonal crystalline phase of the Xe@**111** complex (see below). Phase-pure triclinic x Xe@**111**·1.5DCE (Supporting Information, Figure S15) could only be obtained by carefully limiting the amount of available xenon, though this limitation led to crystals with $x < 1$. TGA-MS analysis of a sample of phase-pure triclinic 0.73Xe@**111**·1.5DCE (Figure 2b) illustrates behavior similar to that of 0.5H₂O@**111**·1.5DCE, except that the onset of DCE loss (ca. 98 °C) is accompanied also by loss of some xenon. The rate of xenon and DCE loss diminishes to almost baseline levels by 140 °C, once the bulk of the DCE is lost, but then increases as the sample is heated through to about 350 °C, at which point an abrupt and final step-wise loss of the remaining xenon and a small amount of residual DCE occurs. The behavior can be explained as follows. The first DCE loss from 0.73Xe@**111**·1.5DCE

instigates a process of structural rearrangement, the dynamics of which allow for rapid evolution of some xenon. According to powder diffraction (PXRD; Supporting Information, Figure S17), the material that results from heating 0.73Xe@**111**·1.5DCE to 140 °C is a mixture of crystalline phases, possibly including the aforementioned trigonal phase. During structural rearrangement, however, some of the xenon is retained and one or more of the new crystalline phases apparently also confine some of the remaining DCE within interstitial sites, the new phases retaining both xenon and DCE at higher temperatures. All of the remaining DCE and xenon are lost in final phase change around 350 °C, which is eventually followed by sublimation, with partial decomposition. ¹H NMR spectroscopy reveals that there is little to no decomposition of **111** under TGA conditions below 375 °C (Supporting Information, Figure S8).

The aforementioned trigonal Xe@**111**· y DCE ($y \leq 1/2$) phase precipitates, in phase-pure form, when a saturated solution of **111** in DCE is treated with xenon gas and left overnight at 80 °C. It precipitates as a fine powder of thin plates and single crystals of sufficient size for SCXRD analysis could not be obtained. A batch, of composition Xe@**111**·0.2DCE prepared in this way was analyzed by ¹H NMR spectroscopy (Supporting Information, Figure S5), TGA-MS, and by PXRD (Supporting Information, Figures S14,S16). NMR spectroscopy revealed a 0.2:1 DCE/**111** ratio; TGA-MS allowed estimation of the xenon content (17.9%, or 0.97Xe@**111**·0.2DCE). The profile shows mass loss in two nearly separate stages. From about 240–290 °C, the mass loss amounting to about 2.9% is almost exclusively DCE (2.4% calc. for Xe@**111**·0.2DCE). From about 290–305 °C, an abrupt, steep mass loss occurs (15.0% obs. vs. 15.5% calc. for the Xe of 0.97Xe@**111**·0.2DCE) concomitant with a solid–solid phase change. MS analysis of the off-gasses shows that a majority of the DCE is lost by the time the MS registers any signal for xenon. Also, heating of Xe@**111**·0.2DCE at 240 °C for one hour under TGA conditions gave a trigonal material completely lacking DCE, but retaining about 0.77 equivalents of xenon (Supporting Information, Figure S7).

Thus, it is clear that trigonal Xe@**111**· y DCE exhibits very high, perhaps unprecedented, kinetic stability. Xenon is retained indefinitely at room temperature, lost only slowly at 240 °C, and the clathrate undergoes rapid decomposition only at temperatures exceeding 290 °C, about 400 °C above the boiling point of xenon. Moreover, the ability of **111** to retain xenon in the solid state is highly structure-dependent; the triclinic phase begins to abruptly lose some xenon at temperatures about 200 °C lower than the trigonal phase. By comparison, β -hydroquinone· x Xe and Xe@Cd-RHO zeolite, both known stable xenon clathrates, begin to abruptly release entrapped xenon at about 132 °C and 200 °C, respectively.^[18a,24] Importantly, despite the high temperatures required to remove xenon from the trigonal solid, the **111** host is easily recovered and recycled. Moreover, the xenon can also be released by simple dissolution of the compound.

To explore the structural factors influencing stability, we determined the structure of trigonal Xe@**111**·0.2DCE by synchrotron PXRD (Supporting Information, Figure S14). The PXRD pattern indexed to a trigonal $R\bar{3}c$ unit cell: $a =$

9.975 Å, $c = 62.321$ Å, $V = 5370.2$ Å³. Structural solution and Rietveld refinement revealed packing of the expanded-conformation Xe@**111** complexes in homochiral layers with the complexes residing on D_3 positions. The structure is akin to the $(ABC)_n$ stacking of cubic close-packed (CCP) spheres (cryptophanes). Adjacent layers of the racemic crystals alternate their Xe@**111** stereochemistry (MM, PP)_n such that six layers are required before the structure repeats, giving a long c -axis (Figure 3). Partial occupancy DCE molecules are

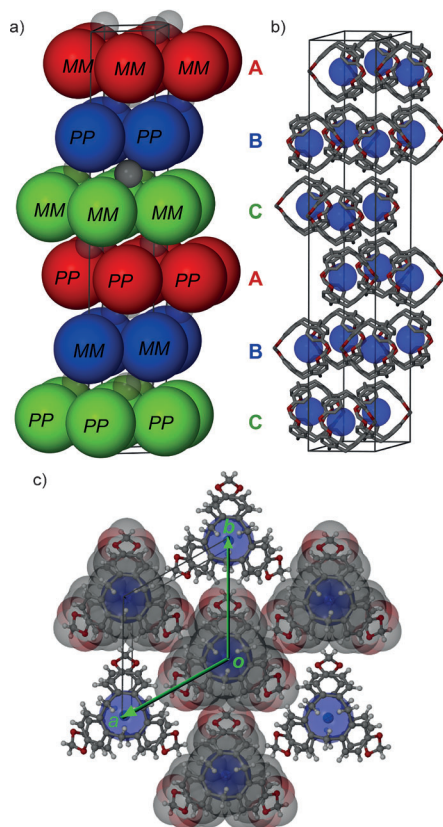


Figure 3. a) Representation of the homochiral, CCP-like $(ABC)_n$ layered packing of trigonal Xe@**111**·0.2DCE. **111** molecules are represented as large spheres, with stereochemistry indicated. Trapped, partial-occupancy DCE molecules are indicated as smaller spheres. b) Identical view as in (a), but illustrating only the Xe@**111** complexes. c) One homochiral layer of Xe@**111** complexes, as viewed down [001], illustrating the nesting of the $-\text{OCH}_2\text{O}-$ bridges in the windows of adjacent Xe@**111** complexes.

disordered in the O_h holes on some of the 3 bar positions. The remarkable stability of the clathrate can be attributed to the high melting point of the solid and the specific high density layer packing, wherein each of the windows of each Xe@**111** complex is completely blocked by the $-\text{OCH}_2\text{O}-$ bridges of adjacent Xe@**111** complexes of the same chirality (Figure 3c). Thus, the potential avenue of escape for Xe is blocked by a conformationally rigid and relatively massive Xe@**111** complex. Interestingly, triclinic Xe@**111**·1.5DCE and $x\text{Xe@111}\cdot 2\text{CHCl}_3$ also adopt layered packing arrangements. In Xe@**111**·1.5DCE, however, the layers are racemic and the complexes pack with a lower density window-to-window

arrangement (Supporting Information, Figure S18). The layers of $x\text{Xe@111}\cdot 2\text{CHCl}_3$, on the other hand, are very similar to that of trigonal Xe@**111**·0.2DCE, but they are racemic. Notably, trigonal Xe@**111**·0.2DCE and $x\text{Xe@111}\cdot 2\text{CHCl}_3$ exhibit approximately the same layer density, suggesting racemic and homochiral layers of similar stability.

To probe Xe/Kr selectivity, attempts were made to synthesize the corresponding krypton clathrates. Interestingly, crystals of triclinic 0.80 Kr@**111**·1.5DCE were easily isolated, but we were unable to synthesize a krypton-containing trigonal phase. No precipitate formed from saturated **111** solutions treated with krypton at 80 °C, implying that selective crystallization of trigonal Xe@**111** may provide a means to separate xenon and krypton. Crystals of 0.80 Kr@**111**·1.5DCE are structurally indistinguishable from Xe@**111**·1.5DCE, including the $\text{Kr}\cdots\text{C}(\text{arene})$ distances (Supporting Information, Tables S2, S6, Figures S11, S13), though the thermal displacement of krypton is slightly larger than the xenon complex. 0.80 Kr@**111**·1.5DCE gives a very similar TGA-MS profile (Figure 2c) as Xe@**111**·1.5DCE except that krypton is more easily lost in the first step.

Finally, sublimation of **111** gave guest-free single crystals, one of which was analyzed by SCXRD. Surprisingly, empty **111** retains its open (and non-collapsed^[25]) conformation ($\tau = 6(4)^\circ$, $\theta = 19(1)^\circ$, $l = 8.4$ Å), with a conformation negligibly different from the H₂O, Kr, and Xe complexes. Therefore, **111** can be regarded as an intrinsically porous material, exhibiting so-called zero-dimensional pores. We suggest that under appropriate conditions (for example, mechanochemical, nanoparticulate, high temperature) these pores may be kinetically accessible to gases and that **111** may be used as a sorbent. Notably, the calculated PXRD pattern of this structure does not match that of the guest-free material obtained after thermally emptying 0.5H₂O@**111**·1.5DCE, indicating that guest-free **111** is polymorphic (Supporting Information, Figure S17).

In conclusion, the discovery of a Xe@**111** crystalline phase of unprecedented stability demonstrates the potential of container molecule materials in the context of gas capture/storage and highlights a need to further study discrete molecule materials exhibiting zero-dimensional pores. In a sense, the **111** pores sit at the opposite end of the pore-accessibility spectrum as compared to, for example, more kinetically accessible xenon-sorbing cage compounds.^[2] It is becoming clear that materials exhibiting empty cryptophanes/cages (for example, polymers,^[17] porous solutions/liquids^[26]) are promising sorbents and/or storage media for various applications involving gas inclusion.

Received: September 23, 2014

Published online: December 11, 2014

Keywords: container molecules · cryptophanes · gas storage · microporous materials · xenon

[1] a) U. Mueller, M. Schubert, F. Teich, H. Puetter, K. Schierle-Arndt, J. Pastré, *J. Mater. Chem.* **2006**, *16*, 626; b) C. A.

- Fernandez, J. Liu, P. K. Thallapally, D. M. Strachan, *J. Am. Chem. Soc.* **2012**, *134*, 9046; c) H. Wang, K. Yao, Z. Zhang, J. Jagiello, Q. Gong, Y. Han, J. Li, *Chem. Sci.* **2014**, *5*, 620; d) B. J. Sikora, C. E. Wilmer, M. L. Greenfield, R. Q. Snurr, *Chem. Sci.* **2012**, *3*, 2217; e) Z. Hulvey, K. V. Lawler, Z. Qiao, J. Zhou, D. Fairen-Jimenez, R. Q. Snurr, S. V. Ushakov, A. Navrotsky, C. M. Brown, P. M. Forster, *J. Phys. Chem. C* **2013**, *117*, 20116; f) T. Ueda, K. Kurokawa, T. Eguchi, C. Kachi-Terajima, S. Takamizawa, *J. Phys. Chem. C* **2007**, *111*, 1524; g) K. V. Lawler, Z. Hulvey, P. M. Forster, *Chem. Commun.* **2013**, *49*, 10959; h) J. Liu, D. M. Strachan, P. K. Thallapally, *Chem. Commun.* **2014**, *50*, 466; i) D. Banerjee, A. J. Cairns, J. Liu, R. K. Motkuri, S. K. Nune, C. A. Fernandez, R. Krishna, D. M. Strachan, P. K. Thallapally, *Acc. Chem. Res.* **2014**, DOI: 10.1021/ar5003126.
- [2] L. Chen, P. S. Reiss, S. Y. Chong, et al., *Nat. Mater.* **2014**, *13*, 954.
- [3] F. G. Kerry, *Industrial Gas Handbook: Gas Separation and Purification*, CRC Press, Boca Raton, **2007**, pp. 129–132.
- [4] J. Izumi in *Handbook of Zeolite Science and Technology* (Eds.: S. M. Auerbach, K. A. Carrado, P. K. Dutta), CRC Press, New York, **2003**, p. 989.
- [5] a) D. Raftery, H. Long, T. Meersmann, P. J. Grandinetti, L. Reven, A. Pines, *Phys. Rev. Lett.* **1991**, *66*, 584; b) I. L. Moudrakovski, A. Nossov, S. Lang, S. R. Breeze, C. I. Ratcliffe, B. Simard, G. Santyr, J. A. Ripmeester, *Chem. Mater.* **2000**, *12*, 1181; c) P. Sozzani, A. Comotti, R. Simonutti, R. Meersmann, J. W. Logan, A. Pines, *Angew. Chem. Int. Ed.* **2000**, *39*, 2695; *Angew. Chem.* **2000**, *112*, 2807; d) A. Comotti, S. Bracco, L. Ferretti, M. Mauri, R. Simonutti, P. Sozzani, *Chem. Commun.* **2007**, 350.
- [6] a) L. Schröder, T. J. Lowery, C. Hilty, D. E. Wemmer, A. Pines, *Science* **2006**, *314*, 446; b) M. M. Spence, S. M. Rubin, I. E. Dimitrov, E. J. Ruiz, D. E. Wemmer, A. Pines, S. Q. Yao, F. Tian, P. G. Schultz, *Proc. Natl. Acad. Sci. USA* **2001**, *98*, 10654; c) P. Berthault, G. Huber, H. Desvaux, *Prog. Nucl. Magn. Reson. Spectrosc.* **2009**, *55*, 35; d) K. K. Palaniappan, M. B. Francis, A. Pines, D. E. Wemmer, *Isr. J. Chem.* **2014**, *54*, 104.
- [7] L. Laureano-Perez, R. Colle, D. R. Jacobson, R. Fitzgerald, N. S. Khan, I. J. Dmochowski, *Appl. Radiat. Isot.* **2012**, *70*, 1997.
- [8] E. J. Karwacki, T. C. Golden, B. Ji, S. A. Motika, T. S. Farris, *Xenon Recovery System*, US Patent 7285154, **2007**.
- [9] a) D. F. Sava, M. A. Rodriguez, K. W. Chapman, P. J. Chupas, J. A. Greathouse, P. S. Crozier, T. M. Nenoff, *J. Am. Chem. Soc.* **2011**, *133*, 12398; b) K. W. Chapman, D. F. Sava, G. J. Halder, P. J. Chupas, T. M. Nenoff, *J. Am. Chem. Soc.* **2011**, *133*, 18583.
- [10] T. Brotin, J. P. Dutasta, *Chem. Rev.* **2009**, *109*, 88.
- [11] K. Bartik, M. Luhmer, J.-P. Dutasta, A. Collet, J. Reisse, *J. Am. Chem. Soc.* **1998**, *120*, 784.
- [12] a) O. Taratula, P. A. Hill, N. S. Khan, P. J. Carroll, I. J. Dmochowski, *Nat. Commun.* **2010**, *1*, 148; b) J. A. Aaron, J. M. Chambers, K. M. Jude, L. Di Costanzo, I. J. Dmochowski, D. W. Christianson, *J. Am. Chem. Soc.* **2008**, *130*, 6942; c) D. R. Jacobson, N. S. Khana, R. Collé, R. Fitzgerald, L. Laureano-Pérez, Y. Baia, I. J. Dmochowski, *Proc. Natl. Acad. Sci. USA* **2011**, *108*, 10969.
- [13] H. A. Fogarty, P. Berthault, T. Brotin, G. Huber, H. Desvaux, J. P. Dutasta, *J. Am. Chem. Soc.* **2007**, *129*, 10332.
- [14] R. M. Fairchild, A. I. Joseph, K. T. Holman, H. A. Fogarty, T. Brotin, J. P. Dutasta, C. Boutin, G. Huber, P. Berthault, *J. Am. Chem. Soc.* **2010**, *132*, 15505.
- [15] a) T. Traoré, L. Delacour, S. Garcia-Argote, P. Berthault, J. C. Cintrat, B. Rousseau, *Org. Lett.* **2010**, *12*, 960; b) T. Traoré, G. Clave, L. Delacour, N. Kotera, P. Y. Renard, A. Romieu, P. Berthault, C. Boutin, N. Tassali, B. Rousseau, *Chem. Commun.* **2011**, *47*, 9702; c) E. Dubost, N. Kotera, S. Garcia-Argote, Y. Boulard, E. Leonce, C. Boutin, P. Berthault, C. Dugave, B. Rousseau, *Org. Lett.* **2013**, *15*, 2866; d) A. I. Joseph, G. El-Ayle, C. Boutin, E. Léonce, P. Berthault, K. T. Holman, *Chem. Commun.* **2014**, *50*, 15905.
- [16] a) J. L. Atwood, L. J. Barbour, A. Jerga, *Science* **2002**, *296*, 2367; b) A. V. Leontiev, D. M. Rudkevich, *Chem. Commun.* **2004**, 1468; c) S. J. Dalgarno, P. K. Thallapally, L. J. Barbour, J. L. Atwood, *Chem. Soc. Rev.* **2007**, *36*, 236; d) A. I. Cooper, *Nat. Chem.* **2010**, *2*, 915.
- [17] a) C. Boulart, M. C. Mowlem, D. P. Connelly, J.-P. Dutasta, C. R. German, *Opt. Express* **2008**, *16*, 12607; b) S. T. Mough, K. T. Holman, *Chem. Commun.* **2008**, 1407.
- [18] a) M. Ilczyszyn, M. Selent, M. M. Ilczyszyn, *J. Phys. Chem. A* **2012**, *116*, 3206; b) G. D. Enright, K. A. Udachin, I. L. Moudrakovski, J. A. Ripmeester, *J. Am. Chem. Soc.* **2003**, *125*, 9896; c) E. B. Brouwer, G. D. Enright, J. A. Ripmeester, *Chem. Commun.* **1997**, 939; d) Y. Miyahara, K. Abe, T. Inazu, *Angew. Chem. Int. Ed.* **2002**, *41*, 3020; *Angew. Chem.* **2002**, *114*, 3146; e) F. Lee, E. Gabe, J. S. Tse, J. A. Ripmeester, *J. Am. Chem. Soc.* **1988**, *110*, 6014; f) S. Takamizawa, T. Akatsuka, T. Ueda, *Angew. Chem. Int. Ed.* **2008**, *47*, 1689; *Angew. Chem.* **2008**, *120*, 1713.
- [19] Unit cell (100 K) of Xe@**111**-2CHCl₃: *Pbcn*, *a* = 50.938(4) Å, *b* = 9.9682(7) Å, *c* = 25.1146(18) Å, *V* = 12752.3(16) Å³.
- [20] K. E. Chaffee, H. A. Fogarty, T. Brotin, B. M. Goodson, J. P. Dutasta, *J. Phys. Chem. A* **2009**, *113*, 13675.
- [21] T. Brupbacher, J. Makarewicz, A. Bauder, *J. Chem. Phys.* **1994**, *101*, 9736.
- [22] S. Mecozzi, J. J. Rebek, *Chem. Eur. J.* **1998**, *4*, 1016.
- [23] D. Cavagnat, T. Brotin, J.-L. Bruneel, J.-P. Dutasta, A. Thozet, M. Perrin, F. Guillaume, *J. Phys. Chem. B* **2004**, *108*, 5572.
- [24] D. R. Corbin, L. Abrams, G. A. Jones, M. L. Smith, C. R. Dybowski, J. A. Hriljacc, J. Parise, *J. Chem. Soc. Chem. Commun.* **1993**, 1027.
- [25] S. T. Mough, J. C. Goeltz, K. T. Holman, *Angew. Chem. Int. Ed.* **2004**, *43*, 5631; *Angew. Chem.* **2004**, *116*, 5749.
- [26] N. O'Reilly, N. Giri, S. L. James, *Chem. Eur. J.* **2007**, *13*, 3020.
- [27] CCDC 924672 (0.8Kr@**111**·1.5DCE), CCDC 924673 (Xe@**111**·1.5DCE), CCDC 924674 (0.5H₂O@**111**·1.5DCE), CCDC 935198 (**111**), and CCDC 1025559 (0.91Xe@**111**·0.2DCE) contain the supplementary crystallographic data for this paper. These data can be obtained free of charge from The Cambridge Crystallographic Data Centre via www.ccdc.cam.ac.uk/data_request/cif.